

**Title Page**

**ATTENUATION OF CISPLATIN-INDUCED RENAL INJURY BY INHIBITION OF  
SOLUBLE EPOXIDE HYDROLASE INVOLVES NF- $\kappa$ B SIGNALING**

Yingmei Liu, Heather K. Webb, Hisayo Fukushima, Janine Micheli, Svetlana Markova,  
Jean L. Olson and Deanna L. Kroetz

Departments of Bioengineering and Therapeutic Sciences (YL, HF, JM, SM and DLK)  
and Anatomic Pathology (JLO), University of California San Francisco, San Francisco,  
CA and Arête Therapeutics, Hayward, CA (HKW)

## Running Title Page

Running title: Soluble epoxide hydrolase and cisplatin nephrotoxicity

Corresponding Author:

Deanna L. Kroetz, Ph.D.

1550 4<sup>th</sup> Street

Box 2911

San Francisco, CA 94158-2911

Tel: 415-476-1159

Fax: 415-514-4361

E-mail: [deanna.kroetz@ucsf.edu](mailto:deanna.kroetz@ucsf.edu)

Number of text pages: 20

Number of Tables: 0

Number of Figures: 8

Number of References: 48

Number of words in Abstract: 205

Number of words in Introduction: 427

Number of words in Discussion: 1574

Abbreviations Used: EETs, epoxyeicosatrienoic acids; DHETs, dihydroxyeicosatrienoic acids; P450, cytochrome P450; sEH, soluble epoxide hydrolase; NF- $\kappa$ B, nuclear factor - $\kappa$ B; iNos, inducible nitric oxide synthase; TNF $\alpha$ , tumor necrosis factor alpha; TNFR1/2,

tumor necrosis factor alpha receptor 1/2; IL-1, interleukin 1; ICAM-1, intercellular adhesive molecule-1; AR9273, 1-adamantan-1-yl-3-(1-methylsulfonyl-piperidin-4-yl-urea); EpOME, epoxyoctadecenoic acid; DiHOME, dihydroxyoctadecenoic acid; Kim-1, kidney injury molecule-1; COX2, cyclooxygenase 2; PPAR $\alpha$ , peroxisome proliferator activated receptor alpha; MAPK, mitogen-activated protein kinase; H&E, hematoxylin and eosin; PAS, periodic acid-schiff ; LC/MS/MS, liquid chromatography-tandem mass spectrometry

Recommended Section Assignment: Toxicology

## Abstract

Acute kidney injury is associated with a significant inflammatory response that has been the target of renoprotection strategies. Epoxyeicosatrienoic acids (EETs) are anti-inflammatory cytochrome P450-derived eicosanoids that are abundantly produced in the kidney and metabolized by soluble epoxide hydrolase (sEH, *Ephx2*) to less active dihydroxyeicosatrienoic acids. Genetic disruption of *Ephx2* and chemical inhibition of sEH were used to test whether the anti-inflammatory effects of EETs, and other lipid epoxide substrates of sEH, afford protection against cisplatin-induced nephrotoxicity. EET hydrolysis was significantly reduced in *Ephx2*<sup>-/-</sup> mice and was associated with an attenuation of cisplatin-induced increases in serum urea and creatinine levels. Histological evidence of renal tubular damage and neutrophil infiltration were also reduced in the *Ephx2*<sup>-/-</sup> mice. Similarly, cisplatin had no effect on renal function, neutrophil infiltration or tubular structure and integrity in mice treated with the potent sEH inhibitor AR9273. Consistent with the ability of EETs to interfere with NF- $\kappa$ B signaling, the observed renoprotection was associated with attenuation of renal NF- $\kappa$ B activity and corresponding decreases in the expression of TNF $\alpha$ , TNFR1, TNFR2 and ICAM-1 prior to the detection of tubular injury. These data suggest that EETs or other fatty acid epoxides can attenuate cisplatin-induced kidney injury and that sEH inhibition is a novel renoprotective strategy.

## Introduction

Acute kidney injury is a common disorder, and a complete understanding of the mechanisms responsible for its development and effective strategies for its prevention or treatment are still lacking. Cisplatin is a widely used broad-spectrum chemotherapeutic that has a dose-limiting renal toxicity associated with high morbidity and mortality (Pabla and Dong, 2008). Nephrotoxic doses of cisplatin lead to a robust induction of proinflammatory cytokines, although the exact mechanism by which cisplatin induces their release and how these cytokines, in turn, contribute to the nephrotoxicity remain unknown (Ramesh and Reeves, 2002; Zhang et al., 2007).

Epoxyeicosatrienoic acids (EETs) are a major product of cytochrome P450 (CYP) epoxygenase-catalyzed arachidonic acid metabolism (Kroetz and Zeldin, 2002). The metabolism of EETs to their corresponding dihydroxyeicosatrienoic acids (DHETs) is catalyzed by soluble epoxide hydrolase (sEH, encoded by *EPHX2*) and this serves as a critical regulatory point for the control of intracellular EET levels. EETs have numerous biological effects in the vasculature and are implicated in the regulation of blood pressure, inflammation and atherosclerosis (Node et al., 1999; Yu et al., 2000b; Schmelzer et al., 2005; Wang et al., 2010). Clinical studies have also suggested that genetic variation in *EPHX2* and CYP epoxygenase genes is associated with an increased risk of coronary heart disease and stroke (Fornage et al., 2004; Lee et al., 2006a; Burdon et al., 2008; Wang et al., 2010; Fava et al., 2011; Lee et al., 2011). In contrast to the increasing impact of EETs and *EPHX2* in vascular biology and disease, little is known about their role in renal injury.

Given the abundance of EET production and degradation in isolated renal tissue and their recognition as vasoprotective and anti-inflammatory molecules (Node et al., 1999; Schmelzer et al., 2005), we hypothesize that renal EETs play a protective role during exposure to nephrotoxic stimuli. Consistent with this hypothesis, a selective sEH inhibitor was recently reported to attenuate cisplatin-induced increases in biochemical markers of renal toxicity, but no mechanistic evidence for the protective effect was provided (Parrish et al., 2008). The objective of this study was to examine the renoprotective properties of lipid epoxides in a well characterized model of acute kidney injury. *Ephx2*<sup>-/-</sup> mice and a novel and selective inhibitor of sEH were used to determine the contribution of lipid epoxides to cisplatin-induced nephrotoxicity. We show that genetic or chemical disruption of sEH activity attenuates the renal damage induced by cisplatin. These effects are attributed to an attenuation of NF- $\kappa$ B signaling and resultant effects on cytokine secretion, adhesion molecule expression and neutrophil infiltration that results from increased intracellular lipid epoxide levels.

## Materials and Methods

### Reagents

Cisplatin was purchased from Aldrich (Milwaukee, WI). The sEH chemical inhibitor AR9273 (1-adamantan-1-yl-3-(1-methylsulfonyl-piperidin-4-yl-urea) was synthesized and kindly provided by Arête Therapeutics (Hayward, CA). An antibody against neutrophils (NIMP-R14) was purchased from Abcam (Cambridge, MA) and goat anti-rat Alexa Fluor 488 antibody was from Molecular Probes (Invitrogen, Carlsbad, CA).

### Animal experiments

C57BL/6 mice were purchased from Charles River Laboratories (Wilmington, MA) and were allowed to acclimate in the animal facility for at least one week prior to use.

*Ephx2*<sup>-/-</sup> mice were originally derived in the Gonzalez laboratory at the National Cancer Institute and were subsequently backcrossed onto a C57BL/6 genetic background for at least seven generations (Sinal et al., 2000). *Ephx2*<sup>-/-</sup> and *Ephx2*<sup>+/+</sup> breeder mice were kindly provided by the Gonzalez laboratory and were subsequently bred in our laboratory. Genotypes were determined in three week old mice using PCR (Sinal et al., 2000). A single 338 bp PCR fragment is detected in *Ephx2*<sup>+/+</sup> mice, a single 295 bp fragment is found in *Ephx2*<sup>-/-</sup> mice, and both fragments are detected in *Ephx2*<sup>+/-</sup> mice (Sinal et al., 2000).

In all studies, eight to ten week old male mice weighing 20-25 g were used. Animal experiments were conducted with adherence to the NIH Guide for the Care and Use of Laboratory Animals and were approved by the Animal Care and Use Committee of the

University of California, San Francisco. Cisplatin and AR9273 were freshly prepared in sterile saline or 1% carboxymethylcellulose/0.1% Tween 80, respectively. C57BL/6 mice were given a daily 100 mg/kg dose of AR9273 or vehicle by oral gavage starting 24 hr prior to and continuing for 24, 48 or 72 hr following cisplatin treatment. Cisplatin was administered as a single intraperitoneal dose of 20 mg/kg and an identical volume of sterile saline was administered to control mice. Mice were housed in metabolic cages for the collection of urine during the 24 hr period prior to sacrifice. Mice were sacrificed at 24, 48 or 72 hr after cisplatin treatment (immediately following the last dose of AR9273). Kidneys were removed and flash frozen in liquid nitrogen. Blood samples were collected via cardiac puncture at the time of sacrifice. All tissue and fluid samples were stored at -80°C until analyzed. In studies involving *Ephx2*<sup>-/-</sup> and *Ephx2*<sup>+/+</sup> littermates, cisplatin treatment and sample collection were carried out exactly as described for the inhibitor studies and samples were collected 72 hr following cisplatin treatment.

### ***TaqMan quantitative PCR***

Total RNA was isolated from kidney tissue using the PARIS kit (Ambion, Austin, TX) according to the manufacturer's instructions. First-strand cDNA was synthesized using SuperScrip III™ reverse transcriptase (Invitrogen, Carlsbad, CA) and any remaining RNA was removed by incubating the samples with 20 U RNase H at 37°C for 15 min. All TaqMan probes and primers were purchased as Assays-on-Demand from Applied Biosystems (Foster City, CA). TaqMan analysis was performed using an Applied Biosystems 7900HT real-time PCR system. Target gene expression was normalized to Gapdh and change in expression was calculated as  $2^{-\Delta\Delta CT}$ , where  $\Delta\Delta CT = (\Delta Ct_{\text{target}} -$

$\Delta Ct_{\text{Gapdh}}^{\text{treated}} - (\Delta Ct_{\text{target}} - \Delta Ct_{\text{Gapdh}}^{\text{control}})$ . PCR conditions were an initial hold at 95°C for 10 min, and then 40 cycles of 95°C for 15 sec and 60°C for 1 min. An equal amount of template cDNA (100 ng) was used for each sample.

### ***Renal function and histology***

Renal function was initially assessed by measurement of serum creatinine and urea nitrogen in the clinical chemistry laboratory at San Francisco General Hospital.

Paraformaldehyde (4%)-fixed and paraffin-embedded kidneys were sectioned at 3  $\mu\text{m}$  and stained with hematoxylin and eosin (H&E) or with periodic acid-Schiff (PAS) using standard methods. All renal histology evaluations were performed by a board certified renal pathologist without knowledge of the experimental groups. Histological changes were evaluated in the cortex and outer stripe of the outer medulla and were scored by counting the numbers of tubules that displayed apoptosis in 20 high power fields (hpf) at 400X magnification. In addition, loss of brush border, cast formation, and tubule dilation were assessed. TUNEL staining was performed on paraffin-embedded kidney samples using an in situ cell death detection kit, TMR red (Roche Diagnostics GmbH, Mannheim, Germany), according to the manufacturer's directions.

Paraffin-embedded kidneys were sectioned at 3  $\mu\text{m}$ . Neutrophils were immunostained with the rat monoclonal NIMP-R14 neutrophil antibody and detected with a goat anti-rat Alexa Fluor 488 antibody. Nuclei were counterstained with DAPI. Images were captured using a Retiga CCD-cooled camera and associated QCapture Pro software (QImaging Surrey, BC Canada). NIMP-R14-positive clusters were counted in ten uniform fields in the cortex and outer medulla of each sample under high power field.

### ***Ex vivo assay of sEH activity***

The ethanol stock solution (1 mg/mL) of the substrate 14,15-EET (Omm Scientific, Dallas, TX), was evaporated to dryness under a stream of nitrogen, and dissolved to 50  $\mu$ M (5X the assay concentration) in assay buffer (0.1 mg/mL bovine serum albumin in 25 mM BisTris, pH 7.0) immediately before the initiation of reactions. Whole blood was diluted 1:10 with 0.1 mg/mL bovine serum albumin in 25 mM BisTris, pH 7.0 and equilibrated to 30°C. The reaction was initiated by the addition of 14,15-EET to a final substrate concentration of 10  $\mu$ M. The reaction was quenched by the addition of 2 volumes of ice-cold methanol and stored at -80°C until analysis by LC/MS/MS. To determine background activity, a control incubation was performed with each sample containing 10  $\mu$ M of the known sEH inhibitor, 12-(3-adamantyl-ureido)-dodecanoic acid (AUDA). The rate of formation of the hydrolysis product, 14,15-dihydroxyeicosatrienoic acid (14,15-DHET) was measured by LC/MS/MS. The sEH specific activity was defined as the rate of product formation, corrected for the background activity.

### ***Quantitation of AR9273 plasma levels***

Blood was collected into EDTA vacutainer tubes from C57BL/6 male mice after dosing either vehicle or AR9273. Plasma was isolated by centrifugation, the samples were mixed with three volumes of 0.1% formic acid in acetonitrile and the precipitates were removed by filtration. AR9273 was quantified in a single run by positive mode electrospray ionization with tandem quadrupole mass spectroscopy.

### ***Oxylipin quantitation***

An API-4000 system was used to determine plasma lipid profiles. Plasma samples were mixed with four volumes of methanol, and the precipitates were removed via filtration. The filtrates were mixed with three plasma volumes of HPLC water. Ten microliter samples were injected onto a diphenyl column (2.1 x 3.3 mm, 2  $\mu$ m) in a gradient run with mobile phase consisting of water and methanol containing 0.2% acetic acid. The lipids were quantified in a single run by negative mode electrospray ionization with tandem quadrupole mass spectroscopy.

### ***NF- $\kappa$ B activity assay and cytokine quantitation***

NF- $\kappa$ B activity was measured using a Quantitation NF- $\kappa$ B EIA kit (Oxford Biomedical Research, Oxford, MI) as described previously (Fife et al., 2008). This chemiluminescence assay employs an oligonucleotide containing the DNA binding NF- $\kappa$ B consensus sequence bound to a 96 well EIA plate. The level of TNF $\alpha$  in the kidney was quantified using a Precoated Mouse TNF $\alpha$  ELISA kit (eBioscience, San Diego, CA) and soluble ICAM-1 (Thermo Scientific, Rockford, IL), TNFR1 and TNFR2 (R&D Systems, Minneapolis, MN) in serum were quantified using EIA kits. Assays were run in duplicate or triplicate exactly as described by the manufacturer. The amount of NF- $\kappa$ B and cytokines were normalized to protein concentration.

### ***Statistics***

Values are expressed as mean  $\pm$  S.D. Data were analyzed by ANOVA followed by Bonferroni post-hoc multiple comparison testing using GraphPad Prism 4.03. A *p* value of < 0.05 was considered significant. All of the analyses were repeated in duplicate or

triplicate using samples from individual animals.

## Results

### ***Genetic disruption of Ephx2 attenuates cisplatin-induced acute kidney injury and cell signaling***

*Ephx2*<sup>-/-</sup> mice were studied to evaluate the role of EETs or other lipid epoxides in cisplatin-induced renal injury. The *Ephx2*<sup>-/-</sup> mice completely lack immunoreactive sEH protein in their kidneys (Supplemental Figure 1). Plasma EpOME/DiHOME ratios are a validated biomarker of in vivo sEH activity (Newman et al., 2002; Luria et al., 2007) and confirmed dramatic inhibition in the *Ephx2*<sup>-/-</sup> mice. EpOME hydrolysis is significantly impaired in the *Ephx2*<sup>-/-</sup> mice, as evident from an increase in EpOME/DiHOME ratios compared to *Ephx2*<sup>+/+</sup> littermates (Figure 1A). The increase in EpOME/DiHOME ratio in the saline-treated *Ephx2*<sup>-/-</sup> mice compared to *Ephx2*<sup>+/+</sup> mice was 2.9- and 78-fold for the 9,10-, and 12,13- ratios, respectively. Similarly, there was a 5.2- and 34-fold increase in the 9,10- and 12,13-EpOME/DiHOME ratios in the cisplatin-treated *Ephx2*<sup>-/-</sup> mice compared to the *Ephx2*<sup>+/+</sup> controls. Treatment of *Ephx2*<sup>+/+</sup> mice with cisplatin resulted in a significant increase in serum urea and creatinine (Figures 1B and 1C). In contrast, identical treatment of *Ephx2*<sup>-/-</sup> mice had no effect on these serum markers of renal function. Histological analysis found only mild tubular injury characterized by mild spotty tubular dilation with rare apoptosis of tubular epithelial cells (35 ± 31 tubules/10 hpf) in cisplatin-treated *Ephx2*<sup>-/-</sup> mice (Figure 1D). Tubular dilation was more widespread in the *Ephx2*<sup>+/+</sup> mice treated with cisplatin. Furthermore, frank tubular epithelial cell necrosis was identified with some sloughed cells within tubular lumina. Casts were also observed. Apoptosis was noted in 92 ± 77 tubules/10 hpf in cisplatin-treated *Ephx2*<sup>+/+</sup> mice ( $p = 0.064$ , *Ephx2*<sup>+/+</sup> vs. *Ephx2*<sup>-/-</sup>). TUNEL staining confirmed a

reduction in cisplatin-induced apoptosis in *Ephx2*<sup>-/-</sup> mice relative to the *Ephx2*<sup>+/+</sup> mice (Figure 2).

An early event in cisplatin-induced renal injury is infiltration of neutrophils into the kidney. Neutrophils were stained with an antibody and visualized by fluorescence microscopy (Figure 1E). The degree of neutrophil infiltration into the cortex induced by cisplatin in *Ephx2*<sup>-/-</sup> mice ( $32 \pm 2.9$  cells/10 hpf) was attenuated in *Ephx2*<sup>-/-</sup> mice ( $21 \pm 2.0$  cells/10 hpf;  $p < 0.05$ , *Ephx2*<sup>+/+</sup> vs. *Ephx2*<sup>-/-</sup>).

The effects of sEH inhibition on TNF $\alpha$  and ICAM-1 gene transcription were measured using TaqMan real-time PCR. The induction of renal TNF $\alpha$  and ICAM-1 mRNA by cisplatin in *Ephx2*<sup>+/+</sup> mice was not evident in *Ephx2*<sup>-/-</sup> mice (Figures 3A and 3B). Consistent with the mRNA results, cisplatin induced renal TNF $\alpha$  and serum ICAM-1 protein levels in *Ephx2*<sup>+/+</sup> mice but not in the *Ephx2*<sup>-/-</sup> mice (Figures 3C and 3D).

### ***Chemical inhibition of sEH attenuates cisplatin-induced renal injury and cell signaling***

A second strategy to evaluate the renoprotective role of EETs or other lipid epoxides in cisplatin-induced acute kidney injury was to treat C57BL/6 mice with AR9273 to inhibit sEH-catalyzed epoxide hydrolysis. The plasma levels of AR9273 shortly after the fifth daily dose ranged from 2.39 - 13.4  $\mu$ M and all animals had levels that were many fold above the IC<sub>50</sub> for mouse sEH of 2.3 nM (data not shown). No AR9273 was detected in vehicle treated animals. Quantitation of EpOME and DiHOME plasma levels confirmed the inhibition of sEH in AR9273-treated mice (Figure 4A). EpOME/DiHOME ratios

increased 8- to 66-fold in mice treated with the sEH inhibitor. The 12,13-EpOME/DiHOME ratio increased to a greater extent (24- and 66-fold in vehicle- and cisplatin-treated mice, respectively) than the 9,10-EpOME/DiHOME ratio (8- and 9-fold in vehicle- and cisplatin-treated mice, respectively). Inhibition of sEH was also demonstrated with an *ex vivo* assay measuring EET hydrolysis in blood collected at 72 hr following cisplatin treatment (data not shown). EET hydrolysis was readily measurable in the plasma of vehicle treated mice but was barely detectable in plasma from AR9273-treated mice.

The effects of 24 - 72 hr treatment with AR9273 on cisplatin-induced renal injury were evaluated by measuring serum creatinine and urea nitrogen levels. AR9273 itself had no effect on serum urea or creatinine and elevation in these markers was not evident until 72 hr after cisplatin treatment (Figures 4B and 4C). Elevation of renal Kim-1 mRNA levels were consistent with renal tubular damage as early as 24 hr after cisplatin treatment (Figure 4D). Histological examination of the kidneys showed no casts and only rare tubular epithelial cell apoptosis in any of the control animals at any time period (Figure 4E). Cisplatin-treated mice showed focal mild tubular dilation with scattered casts and tubular epithelial cell apoptosis (Figure 4E). The extent of tubular epithelial cell necrosis increased over the three days in response to cisplatin treatment, from  $7.2 \pm 2.9$  apoptotic tubule cells/20 hpf at 24 hr to  $89 \pm 21$  apoptotic tubule cells/20 hpf at 72 hr in the cortex ( $p < 0.001$ ). At earlier times single cell apoptosis was noted but by day three, clusters of apoptotic cells were seen. A similar trend was observed in the outer stripe of the outer medulla although the number of affected tubules was less. It should also be noted that the apoptosis in the medulla was seen largely in collecting ducts

whereas proximal and distal tubules as well as collecting ducts showed injury in the cortex. These changes were significantly attenuated in AR9273-treated mice, affecting  $34 \pm 24$  apoptotic tubules/20 hpf at 72 hr ( $p < 0.001$  compared to saline-treated mice at 72 hr). Consistent with the histological analysis, TUNEL staining indicated a significant reduction in cisplatin-induced apoptosis in the presence of AR9273 (Figure 5).

Neutrophils were stained as an early measure of inflammation in response to cisplatin treatment. The majority of neutrophils were found in the glomeruli of cisplatin-treated mice (Figure 4F;  $3.6 \pm 2.1$ ,  $9.4 \pm 9.2$ , and  $19.4 \pm 10.6$  cells/10 hpf at 24, 48 and 72 hr after cisplatin treatment, respectively). Treatment with AR9273 reduced neutrophil infiltration at 48 and 72 hr post treatment to  $3.0 \pm 2.2$  and  $9.1 \pm 8.6$  cells cells/10 hpf, respectively ( $p < 0.05$  for difference at 72 hr). In contrast, minimal neutrophil infiltration was detected in mice treated only with saline or inhibitor ( $< 4.0 \pm 1.0$  cells/10 hpf 24-72 hr after treatment).

Cisplatin treatment resulted in an increase in the renal mRNA levels of  $\text{TNF}\alpha$  (Figure 6A) and ICAM-1 (Figure 6B) within 48 hr of treatment. In both cases, AR9273 administration greatly attenuated this inflammatory response to cisplatin. Renal  $\text{TNF}\alpha$  protein levels were not significantly elevated until 72 hr following cisplatin treatment and this increase was also prevented by AR9273 treatment (Figure 6C). In contrast, a significant increase in soluble ICAM-1 levels in plasma was evident within 24 hr of cisplatin treatment and remained elevated throughout the 72 hr treatment period; this effect was attenuated by sEH inhibition (Figure 6D).

TNF receptors are also regulated by cisplatin signaling and serum levels were

measured. As shown in Figure 7, soluble TNFR1 and TNFR2 levels were dramatically elevated following treatment with cisplatin. In the case of TNFR1, this was evident within 48 hr of treatment while TNFR2 levels were increased already at 24 hr following cisplatin. The levels of both TNF receptors were dramatically attenuated by AR9273 treatment. Similarly, genetic disruption of *Ephx2* provided protection against cisplatin-induced TNFR elevations (Figure 7).

### ***Renoprotective effects of sEH inhibition involve NF- $\kappa$ B signaling***

Based on the effects of sEH inhibition on TNF $\alpha$  signaling and ICAM-1 expression and the known NF- $\kappa$ B inhibitory properties of EETs, we examined NF- $\kappa$ B activation in *Ephx2*<sup>-/-</sup> and AR9273-treated mice. Compared to littermate *Ephx2*<sup>+/+</sup> mice, the basal level of active NF- $\kappa$ B was lower in *Ephx2*<sup>-/-</sup> mice but this did not reach statistical significance (Figure 8A). Cisplatin significantly increased NF- $\kappa$ B activity in *Ephx2*<sup>+/+</sup> mice but not in the *Ephx2*<sup>-/-</sup> mice. Consistent with the findings in *Ephx2*<sup>-/-</sup> mice, chemical inhibition of sEH attenuated the cisplatin-induced increase in NF- $\kappa$ B activity at 72 hr (Figure 8B).

## Discussion

Cisplatin induces acute kidney injury in both animals and humans, and tissue injury is preceded by a robust inflammatory response (Kelly et al., 1999; Deng et al., 2001; Ramesh and Reeves, 2002; Ramesh and Reeves, 2004). An early response to cisplatin treatment includes increases in NF- $\kappa$ B signaling and corresponding induction of TNF $\alpha$  and ICAM-1 expression. Recent studies of modalities that increase EETs, such as *Ephx2*  $-/-$  mice and inhibitors of sEH, suggest that EETs can antagonize inflammatory changes in endothelial cells and in systemic models of inflammation (Node et al., 1999; Fleming et al., 2001; Schmelzer et al., 2005; Smith et al., 2005; Luria et al., 2007; Manhiani et al., 2009; Liu et al., 2010). The anti-inflammatory effects of EETs are attributed, at least in part, to interruption of NF- $\kappa$ B signaling and decreased expression of inflammatory markers such as adhesion molecules and cytokines (Node et al., 1999; Fleming et al., 2001; Schmelzer et al., 2005; Manhiani et al., 2009; Liu et al., 2010). Based on our knowledge of EET action and the pattern of cisplatin nephrotoxicity, we hypothesized that increased intracellular EET levels would attenuate the nephrotoxic effects of cisplatin.

Potential strategies for increasing EET levels include induction of CYP epoxygenases, treatment with EETs or EET mimetics, or inhibition of EET hydrolysis. CYP epoxygenases are induced by dietary fatty acids and during hypertension, but there is no evidence for selective induction of these enzymes by small molecules, including cisplatin (Yu et al., 2000a; Yu et al., 2006). Induction of CYP epoxygenases as a viable approach for increasing EETs is therefore of limited use. Similarly, treatment with EETs

is complicated by their rapid degradation (Spector et al., 2004). While EET mimetics have been designed and are biologically active in vitro or in situ, their use in vivo has not been demonstrated (Yang et al., 2007b). Inhibition of EET hydrolysis is therefore the most attractive approach for increasing EET levels in vivo.

*Ephx2*<sup>-/-</sup> mice were used as one model of increased EET levels. Genetic disruption of sEH activity has previously been used to explore the role of EETs in blood pressure, cardioprotection, systemic inflammation, heart failure, diabetes and vascular remodeling (Seubert et al., 2006; Luria et al., 2007; Monti et al., 2008; Luo et al., 2010; Simpkins et al., 2010). A series of potent and selective inhibitors of sEH have also been synthesized and several have been tested in animal and cellular models (Yu et al., 2000b; Davis et al., 2002; Imig et al., 2002; Zhao et al., 2004; Imig et al., 2005; Schmelzer et al., 2005; Smith et al., 2005; Luria et al., 2007). The current study used a potent and selective inhibitor of lipid epoxide hydrolase activity, AR9273, selected for use in this study due to its oral bioavailability and the resulting changes in the plasma oxylipid ratios it affords in mice. Daily oral treatment of mice with AR9273 results in almost complete inhibition of sEH, as reflected by an ex vivo assay of EET hydrolysis and plasma EpOME/DiHOME ratios. The level of EETs and DHETs in plasma samples from individual mice is close to the limit of detection of the LC/MS/MS assay, but it has previously been shown that the corresponding levels of the C18 fatty acid epoxides and diols, EpOMEs and DiHOMEs, reflect the levels of EETs and DHETs (Newman et al., 2002; Luria et al., 2007). In addition to epoxide hydrolase activity, sEH also has phosphatase activity, which is not affected by AR9273. The inhibitor therefore allows us to focus specifically on the role of EETs and other lipid epoxides, while the *Ephx2*<sup>-/-</sup>

mice informs us about both the epoxide hydrolase and phosphatase activities of sEH. Relatively little is known about the biological effects of other fatty acid epoxide substrates of sEH, and it is possible that multiple oxylipins have renoprotective properties similar to those attributed to the EETs.

Genetic disruption of *Ephx2* or the treatment of mice with a sEH inhibitor was associated with an almost complete attenuation of cisplatin-induced renal damage, measured either as elevations in plasma or renal biomarkers of renal injury, histological changes in renal tubular structure, or neutrophil infiltration. The combined strategy of chemical and genetic disruption of sEH activity provides strong evidence for a renoprotective role for fatty acid epoxides during cisplatin exposure. Importantly, renoprotective effects of the potent sEH inhibitor AR9273 were evident within 24 hr of cisplatin treatment, as measured by the early renal injury biomarker Kim-1, changes in tubular structure, neutrophil infiltration and the number of apoptotic cells. Consistent with these findings, the effects of sEH inhibition on cytokine and adhesion molecule expression were also observed 24 -48 hr before effects of cisplatin on serum creatinine and urea were apparent at 72 hr post treatment. While these data were being analyzed, a report was published showing that the sEH inhibitor 12-(3-adamantan-1-yl-ureido)-dodecanoic acid (AUDA) prevented cisplatin-induced increases in blood urea nitrogen and tubular necrosis (Parrish et al., 2008). Our results confirm and extend these recent findings using a novel sEH inhibitor together with *Ephx2*<sup>-/-</sup> mice. We also provide evidence for an effect of inhibition of sEH hydrolase activity or genetic disruption of *Ephx2* on NF- $\kappa$ B signaling in response to cisplatin. AR9273 had no significant effect on the function of renal transporters involved in cisplatin uptake (data not shown), providing

further support that the observed renoprotective effects are a result of changes in EET degradation by sEH.

Our findings are consistent with the widely accepted major role for TNF $\alpha$  in mediating a robust inflammatory response to cisplatin treatment (Deng et al., 2001; Ramesh and Reeves, 2002; Ramesh and Reeves, 2004; Li et al., 2005; Lee et al., 2006b; Zhang et al., 2007). Increased TNF $\alpha$  levels were an early response to cisplatin. Both TNFR1 and TNFR2 have been implicated in cisplatin-induced TNF $\alpha$  signaling. Studies in TNFR1-deficient mice have shown that signaling through TNFR1 is involved in tubular cell apoptosis following cisplatin treatment (Tsuruya et al., 2003). In contrast, others have shown that TNFR2 plays a more important role than TNFR1 in mediating the inflammatory and apoptotic effects of cisplatin, including ICAM-1 induction (Ramesh and Reeves, 2003). The fact that sEH inhibition can inhibit both TNFR2 and ICAM-1 induction to a similar degree and time dependency is consistent with EETs interfering with this signaling pathway. In the current study, cisplatin induced a more dramatic increase in circulating TNFR1 levels compared to TNFR2. Importantly, the induction of both TNFR1 and TNFR2 was an early response to cisplatin treatment, and evident within 24 hr of treatment. The more dramatic effect on cisplatin-induced apoptosis compared to neutrophil infiltration is consistent with the significant changes in TNFR1 expression. The ability of sEH inhibition to attenuate these early increases in TNF $\alpha$  and soluble TNFR expression suggests that this could be an effective strategy for ameliorating both the inflammatory and apoptotic effects of cisplatin. This is significant since previous studies focused on inhibition of inflammation alone did not prevent cisplatin-induced renal injury (Faubel et al., 2007).

The induction of renal NF- $\kappa$ B activity by cisplatin was also prevented by inhibition of sEH activity, and is consistent with the ability of EETs to disrupt NF- $\kappa$ B signaling (Node et al., 1999). In endothelial cells, EETs interfere with NF- $\kappa$ B signaling by disrupting I $\kappa$ B kinase activity, resulting in decreased expression of proinflammatory proteins (Node et al., 1999). Consistent with these findings in isolated cells, the induction in mice of the proinflammatory proteins COX-2 and iNOS by endotoxin treatment is attenuated by sEH inhibition (Schmelzer et al., 2005). Similarly, acute exposure to tobacco smoke results in inflammatory cell infiltration into bronchial lavage fluid, a response that is greatly attenuated by treatment with a sEH inhibitor (Smith et al., 2005). The effect of sEH inhibition on cisplatin-induced changes in renal NF- $\kappa$ B activity is similar to the effect of salicylate, fibrate or rosiglitazone treatment in this model (Ramesh and Reeves, 2004; Li et al., 2005; Lee et al., 2006b). In all cases, the attenuation of NF- $\kappa$ B activity is almost complete, supporting a critical role for these molecules in cisplatin nephrotoxicity.

NF- $\kappa$ B signaling is implicated in the regulation of both TNF $\alpha$  and TNFR2. TNF $\alpha$  itself can activate I $\kappa$ B kinase, leading to NF- $\kappa$ B activity (Kelliher et al., 1998). Both TNFR2 and TNF $\alpha$  have NF- $\kappa$ B binding sites which could account for their induction in response to cisplatin treatment (Santee and Owen-Schaub, 1996; Yao et al., 1997). Further downstream effects of NF- $\kappa$ B activation include induction of ICAM-1 and subsequent neutrophil infiltration (Ramesh and Reeves, 2002; Ramesh and Reeves, 2003; Francescato et al., 2007). The ability of EETs to interfere with NF- $\kappa$ B signaling is consistent with the findings that sEH inhibition attenuates the effect of cisplatin on TNF $\alpha$ , TNFR and ICAM-1 expression and provides a plausible mechanism for the

observed renoprotection afforded by sEH inhibition.

Collectively, these data provide convincing evidence that sEH inhibition protects against cisplatin-induced renal injury, at least in part by attenuation of NF- $\kappa$ B signaling. In addition to their interaction with the NF- $\kappa$ B signaling pathway, EETs also interfere with other signaling pathways implicated in cisplatin toxicity, including PPAR $\alpha$  and MAPK (Ng et al., 2007; Yang et al., 2007a). Whether these signaling pathways are involved in the renoprotective effects of sEH inhibition require further study. It will also be of interest to explore whether renoprotection by EETs is afforded in other models of acute kidney injury, such as ischemia reperfusion and mechanical injury. sEH inhibition does protect against renal injury associated with salt-sensitive hypertension, but in this case it is hard to determine the contribution of lowering blood pressure to the observed effects (Imig et al., 2005; Manhiani et al., 2009). Indeed, combined effects of EETs on inflammatory signaling and vasoactivity may enhance the therapeutic potential of sEH inhibition for renoprotection.

## **Acknowledgments**

We acknowledge Julie Siegenthaller for her assistance with neutrophil image capture and useful discussions.

## Authorship Contributions

Participated in research design: Liu, Webb, Olson and Kroetz

Conducted experiments: Liu, Fukushima, Micheli and Markova

Contributed new reagents or analytic tools: none

Performed data analysis: Liu, Fukushima and Kroetz

Wrote or contributed to the writing of the manuscript: Liu, Fukushima, Micheli, Markova,  
Webb, Olson and Kroetz

## References

- Burdon KP, Lehtinen AB, Langefeld CD, Carr JJ, Rich SS, Freedman BI, Herrington D and Bowden DW (2008) Genetic analysis of the soluble epoxide hydrolase gene, EPHX2, in subclinical cardiovascular disease in the Diabetes Heart Study. *Diab Vasc Dis Res* **5**:128-134.
- Davis BB, Thompson DA, Howard LL, Morisseau C, Hammock BD and Weiss RH (2002) Inhibitors of soluble epoxide hydrolase attenuate vascular smooth muscle cell proliferation. *Proc Natl Acad Sci USA* **99**:2222-2227.
- Deng J, Kohda Y, Chiao H, Wang Y, Hu X, Hewitt SM, Miyaji T, McLeroy P, Nibhanupudy B, Li S and Star RA (2001) Interleukin-10 inhibits ischemic and cisplatin-induced acute renal injury. *Kidney Int* **60**:2118-2128.
- Faubel S, Lewis EC, Reznikov L, Ljubanovic D, Hoke TS, Somerset H, Oh DJ, Lu L, Klein CL, Dinarello CA and Edelstein CL (2007) Cisplatin-induced acute renal failure is associated with an increase in the cytokines interleukin (IL)-1beta, IL-18, IL-6, and neutrophil infiltration in the kidney. *J Pharmacol Exp Ther* **322**:8-15.
- Fava C, Montagnana M, Danese E, Almgren P, Hedblad B, Engstrom G, Berglund G, Minuz P and Melander O (2011) Homozygosity for the EPHX2 K55R polymorphism increases the long-term risk of ischemic stroke in men: a study in Swedes. *Pharmacogenet Genomics* **20**:94-103.
- Fife KL, Liu Y, Schmelzer KR, Tsai HJ, Kim IH, Morisseau C, Hammock BD and Kroetz DL (2008) Inhibition of soluble epoxide hydrolase does not protect against endotoxin-mediated hepatic inflammation. *J Pharmacol Exp Ther* **327**:707-715.
- Fleming I, Michaelis UR, Bredenkotter D, Fisslthaler B, Dehghani F, Brandes RP and

Busse R (2001) Endothelium-derived hyperpolarizing factor synthase (Cytochrome P450 2C9) is a functionally significant source of reactive oxygen species in coronary arteries. *Circ Res* **88**:44-51.

Fornage M, Boerwinkle E, Doris PA, Jacobs D, Liu K and Wong ND (2004)

Polymorphism of the soluble epoxide hydrolase is associated with coronary artery calcification in African-American subjects: The Coronary Artery Risk Development in Young Adults (CARDIA) study. *Circulation* **109**:335-339.

Francescato HD, Costa RS, Scavone C and Coimbra TM (2007) Parthenolide reduces cisplatin-induced renal damage. *Toxicology* **230**:64-75.

Imig JD, Zhao X, Capdevila JH, Morisseau C and Hammock BD (2002) Soluble epoxide hydrolase inhibition lowers arterial blood pressure in angiotensin II hypertension.

*Hypertension* **39**:690-694.

Imig JD, Zhao X, Zaharis CZ, Olearczyk JJ, Pollock DM, Newman JW, Kim IH,

Watanabe T and Hammock BD (2005) An orally active epoxide hydrolase inhibitor lowers blood pressure and provides renal protection in salt-sensitive hypertension.

*Hypertension* **46**:975-981.

Kelliher MA, Grimm S, Ishida Y, Kuo F, Stanger BZ and Leder P (1998) The death domain kinase RIP mediates the TNF-induced NF-kappaB signal. *Immunity* **8**:297-303.

Kelly KJ, Meehan SM, Colvin RB, Williams WW and Bonventre JV (1999) Protection from toxicant-mediated renal injury in the rat with anti-CD54 antibody. *Kidney Int* **56**:922-931.

Kroetz DL and Zeldin DC (2002) Cytochrome P450 pathways of arachidonic acid

metabolism. *Curr Opin Lipidol* **13**:273-283.

Lee CR, North KE, Bray MS, Fornage M, Seubert JM, Newman JW, Hammock BD, Couper DJ, Heiss G and Zeldin DC (2006a) Genetic variation in soluble epoxide hydrolase (EPHX2) and risk of coronary heart disease: The Atherosclerosis Risk in Communities (ARIC) study. *Hum Mol Genet* **15**:1640-1649.

Lee CR, Pretorius M, Schuck RN, Burch LH, Bartlett J, Williams SM, Zeldin DC and Brown NJ (2011) Genetic variation in soluble epoxide hydrolase (EPHX2) is associated with forearm vasodilator responses in humans. *Hypertension* **57**:116-122.

Lee S, Kim W, Moon SO, Sung MJ, Kim DH, Kang KP, Jang YB, Lee JE, Jang KY and Park SK (2006b) Rosiglitazone ameliorates cisplatin-induced renal injury in mice. *Nephrol Dial Transplant* **21**:2096-2105.

Li S, Gokden N, Okusa MD, Bhatt R and Portilla D (2005) Anti-inflammatory effect of fibrate protects from cisplatin-induced ARF. *Am J Physiol Renal Physiol* **289**:F469-480.

Liu JY, Yang J, Inceoglu B, Qiu H, Ulu A, Hwang SH, Chiamvimonvat N and Hammock BD (2010) Inhibition of soluble epoxide hydrolase enhances the anti-inflammatory effects of aspirin and 5-lipoxygenase activation protein inhibitor in a murine model. *Biochem Pharmacol* **79**:880-887.

Luo P, Chang HH, Zhou Y, Zhang S, Hwang SH, Morisseau C, Wang CY, Inscho EW, Hammock BD and Wang MH (2010) Inhibition or deletion of soluble epoxide hydrolase prevents hyperglycemia, promotes insulin secretion, and reduces islet apoptosis. *J Pharmacol Exp Ther* **334**:430-438.

- Luria A, Weldon SM, Kabcenell AK, Ingraham RH, Matera D, Jiang H, Gill R, Morisseau C, Newman JW and Hammock BD (2007) Compensatory mechanism for homeostatic blood pressure regulation in *Ephx2* gene-disrupted mice. *J Biol Chem* **282**:2891-2898.
- Manhiani M, Quigley JE, Knight SF, Tasoobshirazi S, Moore T, Brands MW, Hammock BD and Imig JD (2009) Soluble epoxide hydrolase gene deletion attenuates renal injury and inflammation with DOCA-salt hypertension. *Am J Physiol Renal Physiol* **297**:F740-748.
- Monti J, Fischer J, Paskas S, Heinig M, Schulz H, Gosele C, Heuser A, Fischer R, Schmidt C, Schirdewan A, Gross V, Hummel O, Maatz H, Patone G, Saar K, Vingron M, Weldon SM, Lindpaintner K, Hammock BD, Rohde K, Dietz R, Cook SA, Schunck WH, Luft FC and Hubner N (2008) Soluble epoxide hydrolase is a susceptibility factor for heart failure in a rat model of human disease. *Nat Genet* **40**:529-537.
- Newman JW, Watanabe T and Hammock BD (2002) The simultaneous quantification of cytochrome P450 dependent linoleate and arachidonate metabolites in urine by HPLC-MS/MS. *J Lipid Res* **43**:1563-1578.
- Ng VY, Huang Y, Reddy LM, Falck JR, Lin ET and Kroetz DL (2007) Cytochrome P450 eicosanoids are activators of peroxisome proliferator-activated receptor alpha (PPAR $\alpha$ ). *Drug Metab Dispos* **35**:1126-1134.
- Node K, Huo Y, Ruan X, Yang B, Spiecker M, Ley K, Zeldin DC and Liao JK (1999) Anti-inflammatory properties of cytochrome P450 epoxygenase-derived eicosanoids. *Science* **285**:1276-1279.

- Pabla N and Dong Z (2008) Cisplatin nephrotoxicity: mechanisms and renoprotective strategies. *Kidney Int* **73**:994-1007.
- Parrish AR, Chen G, Burghardt RC, Watanabe T, Morisseau C and Hammock BD (2008) Attenuation of cisplatin nephrotoxicity by inhibition of soluble epoxide hydrolase. *Cell Biol Toxicol* **25**:217-225.
- Ramesh G and Reeves WB (2002) TNF- $\alpha$  mediates chemokine and cytokine expression and renal injury in cisplatin nephrotoxicity. *J Clin Invest* **110**:835-842.
- Ramesh G and Reeves WB (2003) TNFR2-mediated apoptosis and necrosis in cisplatin-induced acute renal failure. *Am J Physiol Renal Physiol* **285**:F610-618.
- Ramesh G and Reeves WB (2004) Salicylate reduces cisplatin nephrotoxicity by inhibition of tumor necrosis factor- $\alpha$ . *Kidney Int* **65**:490-499.
- Santee SM and Owen-Schaub LB (1996) Human tumor necrosis factor receptor p75/80 (CD120b) gene structure and promoter characterization. *J Biol Chem* **271**:21151-21159.
- Schmelzer KR, Kubala L, Newman JW, Kim IH, Eiserich JP and Hammock BD (2005) Soluble epoxide hydrolase is a therapeutic target for acute inflammation. *Proc Natl Acad Sci U S A* **102**:9772-9777.
- Seubert JM, Sinal CJ, Graves J, DeGraff LM, Bradbury JA, Lee CR, Goralski K, Carey MA, Luria A, Newman JW, Hammock BD, Falck JR, Roberts H, Rockman HA, Murphy E and Zeldin DC (2006) Role of soluble epoxide hydrolase in postischemic recovery of heart contractile function. *Circ Res* **99**:442-450.
- Simpkins AN, Rudic RD, Roy S, Tsai HJ, Hammock BD and Imig JD (2010) Soluble epoxide hydrolase inhibition modulates vascular remodeling. *Am J Physiol Heart*

*Circ Physiol* **298**:H795-806.

Sinal CJ, Miyata M, Tohkin M, Nagata K, Bend JR and Gonzalez FJ (2000) Targeted disruption of soluble epoxide hydrolase reveals a role in blood pressure regulation. *J Biol Chem* **275**:40504-40510.

Smith KR, Pinkerton KE, Watanabe T, Pedersen TL, Ma SJ and Hammock BD (2005) Attenuation of tobacco smoke-induced lung inflammation by treatment with a soluble epoxide hydrolase inhibitor. *Proc Natl Acad Sci U S A* **102**:2186-2191.

Spector AA, Fang X, Snyder GD and Weintraub NL (2004) Epoxyeicosatrienoic acids (EETs): metabolism and biochemical function. *Prog Lipid Res* **43**:55-90.

Tsuruya K, Ninomiya T, Tokumoto M, Hirakawa M, Masutani K, Taniguchi M, Fukuda K, Kanai H, Kishihara K, Hirakata H and Iida M (2003) Direct involvement of the receptor-mediated apoptotic pathways in cisplatin-induced renal tubular cell death. *Kidney Int* **63**:72-82.

Wang YX, Ulu A, Zhang LN and Hammock B (2010) Soluble epoxide hydrolase in atherosclerosis. *Current atherosclerosis reports* **12**:174-183.

Yang S, Lin L, Chen JX, Lee CR, Seubert JM, Wang Y, Wang H, Chao ZR, Tao DD, Gong JP, Lu ZY, Wang DW and Zeldin DC (2007a) Cytochrome P-450 epoxygenases protect endothelial cells from apoptosis induced by tumor necrosis factor- $\alpha$  via MAPK and PI3K/Akt signaling pathways. *Am J Physiol Heart Circ Physiol* **293**:H142-151.

Yang W, Holmes BB, Gopal VR, Kishore RV, Sangras B, Yi XY, Falck JR and Campbell WB (2007b) Characterization of 14,15-epoxyeicosatrienoyl-sulfonamides as 14,15-epoxyeicosatrienoic acid agonists: use for studies of metabolism and ligand binding.

*J Pharmacol Exp Ther* **321**:1023-1031.

Yao J, Mackman N, Edgington TS and Fan ST (1997) Lipopolysaccharide induction of the tumor necrosis factor- $\alpha$  promoter in human monocytic cells. Regulation by Egr-1, c-Jun, and NF- $\kappa$ B transcription factors. *J Biol Chem* **272**:17795-17801.

Yu Z, Huse LM, Adler P, Graham L, Ma J, Zeldin DC and Kroetz DL (2000a) Increased CYP2J expression and epoxyeicosatrienoic acid formation in spontaneously hypertensive rat kidney. *Mol Pharmacol* **57**:1011-1020.

Yu Z, Ng VY, Su P, Engler MM, Engler MB, Huang Y, Lin E and Kroetz DL (2006) Induction of renal cytochrome P450 arachidonic acid epoxygenase activity by dietary  $\gamma$ -linolenic acid. *J Pharmacol Exp Ther* **317**:732-738.

Yu Z, Xu F, Huse LM, Morisseau C, Draper AJ, Newman JW, Parker C, Graham L, Engler MM, Hammock BD, Zeldin DC and Kroetz DL (2000b) Soluble epoxide hydrolase regulates hydrolysis of vasoactive epoxyeicosatrienoic acids. *Circ Res* **87**:992-998.

Zhang B, Ramesh G, Norbury CC and Reeves WB (2007) Cisplatin-induced nephrotoxicity is mediated by tumor necrosis factor- $\alpha$  produced by renal parenchymal cells. *Kidney Int* **72**:37-44.

Zhao X, Yamamoto T, Newman JW, Kim IH, Watanabe T, Hammock BD, Stewart J, Pollock JS, Pollock DM and Imig JD (2004) Soluble epoxide hydrolase inhibition protects the kidney from hypertension-induced damage. *J Am Soc Nephrol* **15**:1244-1253.

## Footnotes

- a) This work was supported by UC Discovery Grant Bio06-1-576, the National Institutes of Health National Institute of Diabetes and Digestive and Kidney Diseases [Grant DK084147], and in part by Arête Therapeutics. Janine Micheli was supported in part by NIH Training Grant T32 GM007175.
  
- b) Reprint requests to: Deanna L. Kroetz, Ph.D., 1550 4<sup>th</sup> Street, Box 2911, San Francisco, CA 94158-2911; email: deanna.kroetz@ucsf.edu.

## Legends for Figures

### **Figure 1. Genetic disruption of *Ephx2* protects against cisplatin-induced acute kidney injury.**

*Ephx2*<sup>+/+</sup> and *Ephx2*<sup>-/-</sup> mice were treated with saline or cisplatin and kidneys and blood were harvested 72 hr later. Plasma EpOME/DiHOME ratios are shown in panel A for the 9,10- (black bars) and 12,13- (hatched bars) regioisomers.

Values shown are the mean  $\pm$  S.D. from five or six mice per treatment group.

Significant differences between *Ephx2*<sup>+/+</sup> and *Ephx2*<sup>-/-</sup> mice are indicated: \* $p < 0.05$

and \*\* $p < 0.01$ . Urea nitrogen (B) and creatinine (C) were measured in serum and

values shown are the mean  $\pm$  S.D. from six mice per group. Significant differences

between vehicle and cisplatin treatment groups are indicated for each strain: \* $p < 0.05$

and \*\*\* $p < 0.001$ . In panel D, representative photomicrographs are shown from vehicle-

and cisplatin-treated *Ephx2*<sup>+/+</sup> and *Ephx2*<sup>-/-</sup> mice. Note tubules containing casts (C) or

sloughed tubular cells in cisplatin-treated *Ephx2*<sup>+/+</sup> kidneys. Apoptotic bodies (arrow)

can also be seen in this group. The remaining groups show little damage. Tissue slices

were stained with PAS and photomicrographs are shown at 400X magnification. In

panel E, neutrophil staining is shown in representative slides from saline- and cisplatin-

treated *Ephx2*<sup>+/+</sup> and *Ephx2*<sup>-/-</sup> mice. Kidney sections (3  $\mu$ m) were immunostained with

a rat monoclonal antibody against neutrophils (bright green) and nuclei were

counterstained with DAPI (blue). Neutrophil clusters are marked with arrows. The bar

indicates 50  $\mu$ m; in the inset the scale bar corresponds to 5  $\mu$ m.

### **Figure 2. Genetic disruption of *Ephx2* protects against cisplatin-induced**

**apoptosis.** Apoptotic cells were detected by TUNEL staining. The bar indicates 100

$\mu\text{m}$ . The number of apoptotic cells were counted in 10 hpf and the mean  $\pm$  SD from three to four mice per group is expressed relative to control kidneys. Significant differences are indicated: \*\*\*  $p < 0.001$ , between vehicle and cisplatin treated mice;  $\dagger p < 0.05$  between cisplatin treated *Ephx2*<sup>+/+</sup> and *Ephx2*<sup>-/-</sup> mice.

**Figure 3. Cisplatin-mediated renal inflammatory gene expression is prevented by genetic disruption of *Ephx2*.** *Ephx2*<sup>+/+</sup> and *Ephx2*<sup>-/-</sup> mice were treated with saline or cisplatin and renal and serum markers of inflammation were measured 72 hr later. TNF $\alpha$  (A) and ICAM-1 (B) mRNA levels were measured in the kidneys of vehicle- and cisplatin-treated *Ephx2*<sup>+/+</sup> and *Ephx2*<sup>-/-</sup> mice by quantitative real-time PCR. RNA levels were normalized to Gapdh and the data is presented as the relative change in expression between vehicle and cisplatin-treated groups. Renal TNF $\alpha$  (C) and serum ICAM-1 (D) protein levels were quantified by EIA. The values shown are the mean  $\pm$  S.D. of five or six mice per treatment group. Significant differences between vehicle and cisplatin treatment in each strain are indicated: \*\* $p < 0.01$  and \*\*\* $p < 0.001$ .

**Figure 4. sEH inhibition prevents cisplatin-induced acute kidney injury in C57BL/6 mice.** Mice were treated daily with 100 mg/kg AR9273 or vehicle for five days and a single dose of 20 mg/kg cisplatin was administered on day two. Kidneys and blood were harvested 24-72 hr after cisplatin treatment and used for characterization of renal injury. Plasma EpOME/DiHOME ratios are shown in panel A for the 9,10- (black bars) and 12,13- (hatched bars) regioisomers. The values represent the mean  $\pm$  S.D. from five to eight samples per treatment group. Significant differences are indicated: \*\*\* $p < 0.001$  between vehicle and AR9273 treated mice;  $\dagger\dagger p < 0.001$  between mice

treated with cisplatin alone and cisplatin with AR9273. Urea nitrogen (B) and creatinine (C) were measured in serum and Kim-1 mRNA levels (D) were measured in renal tissue. The values shown are the mean  $\pm$  S.D. from eight to ten mice per group. The renal Kim-1 mRNA levels are expressed relative to vehicle treated mice. Significant differences are indicated:  $**p < 0.01$  and  $***p < 0.001$  between vehicle and cisplatin treated mice;  $^{\dagger\dagger}p < 0.01$  and  $^{\dagger\dagger\dagger}p < 0.001$  between mice treated with cisplatin alone and cisplatin with AR9273. In panel E, kidney slices were stained with PAS and representative photomicrographs are shown at 400X magnification. At 24 hours little difference is seen between the mice treated with cisplatin alone and cisplatin treated with AR9273. At 48 hours an increase in the number of apoptotic bodies (arrows) is identified in the mice treated with cisplatin alone. At 72 hours note the presence of casts and frank tubular necrosis in the groups treated with cisplatin alone. In addition, clusters of apoptotic bodies are seen as compared to the single apoptotic cells seen in the other groups. In panel F, kidney sections (3  $\mu\text{m}$ ) were immunostained with a rat monoclonal antibody against neutrophils (bright green) and nuclei were stained with DAPI (blue). Neutrophil clusters are marked with arrows. The bar indicates 50  $\mu\text{m}$ ; in the inset the scale bar corresponds to 5  $\mu\text{m}$ .

**Figure 5. sEH inhibition protects against cisplatin-induced apoptosis.** Apoptotic cells were detected by TUNEL staining. The bar indicates 100  $\mu\text{m}$ . The number of apoptotic cells were counted in 10 hpf and the mean  $\pm$  SD from three to four mice per group is expressed relative to control kidneys. Significant differences are indicated:  $***p < 0.001$ , between vehicle and cisplatin treated mice;  $^{\dagger}p < 0.05$  between mice treated with cisplatin alone and cisplatin with AR9273.

**Figure 6. Cisplatin-mediated renal inflammatory gene expression is attenuated by inhibition of soluble epoxide hydrolase.** Mice were treated daily with 100 mg/kg AR9273 or vehicle orally for five days and a single dose of 20 mg/kg cisplatin was administered on day two. Kidneys and blood were harvested 24-72 hr after cisplatin treatment and used for measurement of inflammatory markers. Renal TNF $\alpha$  (A) and ICAM-1 (B) mRNA levels were measured by quantitative real-time PCR. RNA levels were normalized to Gapdh and the data is presented relative to the vehicle-treated group. Renal TNF $\alpha$  (C) and serum ICAM-1 (D) protein levels were quantified by EIA. The values shown are the mean  $\pm$  S.D. of eight to ten mice per treatment group. Significant differences are indicated: \* $p < 0.05$ , \*\* $p < 0.01$  and \*\*\* $p < 0.001$  between vehicle and cisplatin treated mice;  $^{\dagger}p < 0.05$ ,  $^{\ddagger}p < 0.01$  and  $^{\dagger\dagger\dagger}p < 0.001$  between mice treated with cisplatin alone and cisplatin with AR9273.

**Figure 7. Cisplatin-mediated induction of sTNFR1 and sTNFR2 is attenuated by genetic disruption of *Ephx2* or inhibition of soluble epoxide hydrolase.** *Ephx2*<sup>+/+</sup> and *Ephx2*<sup>-/-</sup> mice were treated with saline or cisplatin and blood was collected 72 hr later (A and B). In other studies, C57BL/6 mice were treated daily with 100 mg/kg AR9273 or vehicle orally for five days and a single dose of 20 mg/kg cisplatin was administered on day two (C and D). Blood was harvested 24-72 hr after cisplatin treatment. sTNFR1 (A and C) and sTNFR2 (B and D) were measured by EIA. Values shown are the mean  $\pm$  S.D. from five mice for each treatment group. Significant differences are indicated: \* $p < 0.05$ , \*\* $p < 0.01$  and \*\*\* $p < 0.001$  between vehicle and cisplatin treated mice;  $^{\ddagger}p < 0.01$  and  $^{\dagger\dagger\dagger}p < 0.001$  between mice treated with cisplatin alone and cisplatin with AR9273.

**Figure 8. Activation of NF- $\kappa$ B is prevented by genetic disruption of *Ephx2* or soluble epoxide hydrolase inhibition.** Renal nuclear lysates collected 72 hr post cisplatin treatment were used for measurement of activated NF- $\kappa$ B. The effect of cisplatin was compared between *Ephx2*<sup>+/+</sup> and *Ephx2*<sup>-/-</sup> mice (A) and in vehicle and AR9273 treated mice (B). Values shown are the mean  $\pm$  S.D. of five or six samples per treatment group. Significant differences are indicated: \* $p < 0.05$  and \*\* $p < 0.01$  for difference between vehicle and cisplatin treatment in *Ephx2*<sup>+/+</sup> and C57BL/6 mice, respectively; <sup>††</sup> $p < 0.01$  for difference between mice treated with cisplatin alone and cisplatin plus AR9273.

Figure 1.

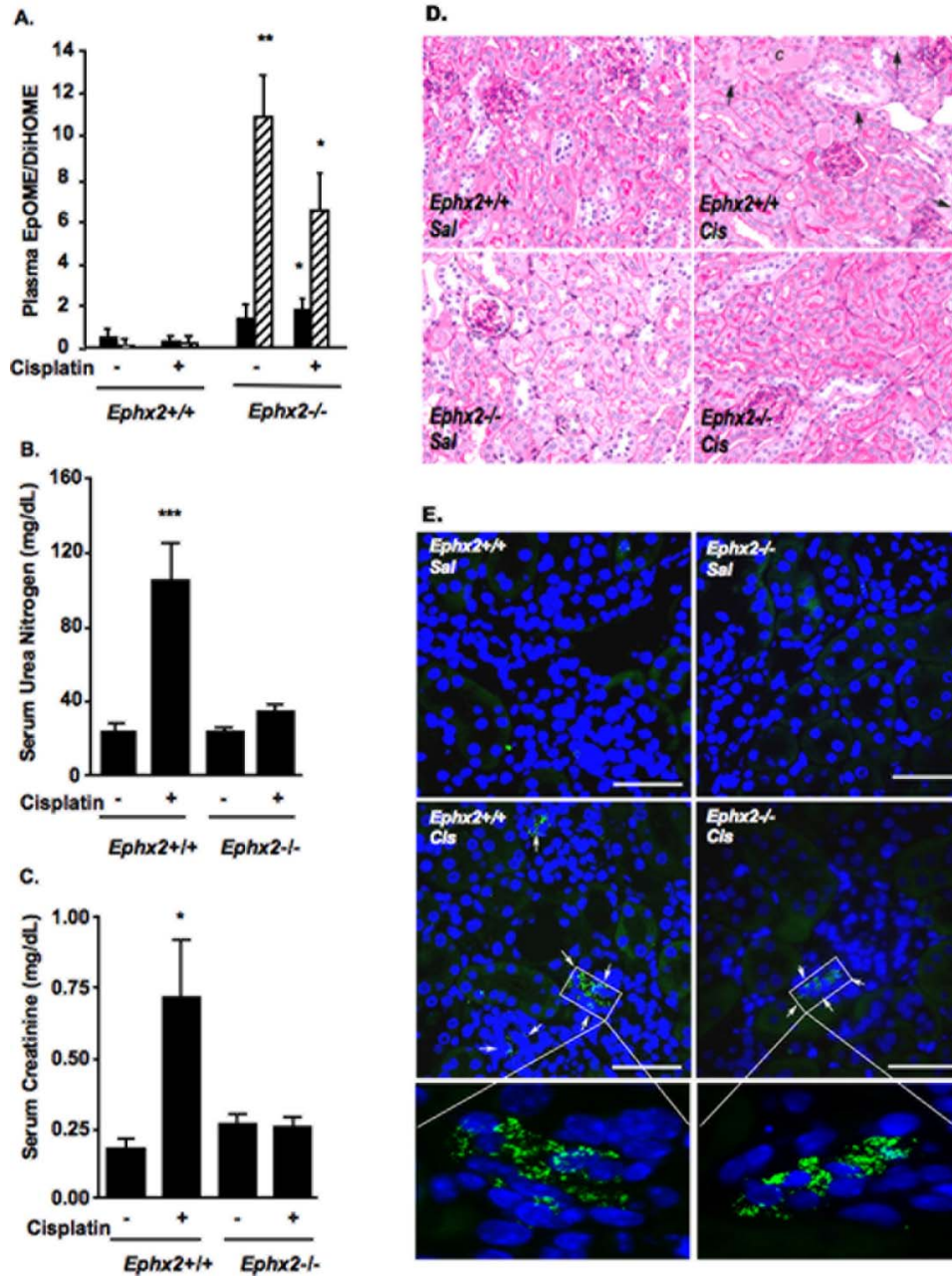


**Figure 2.**

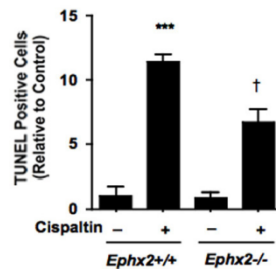
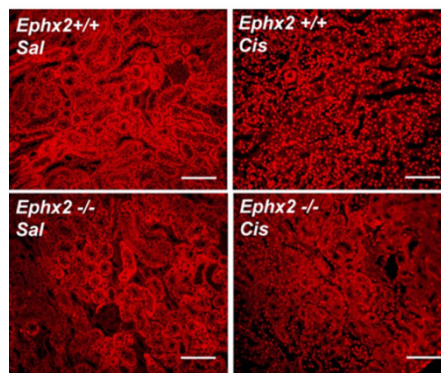


Figure 3.

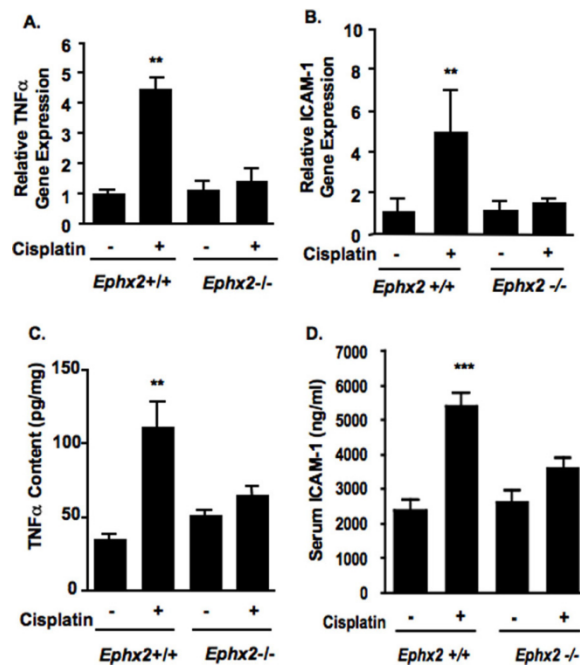
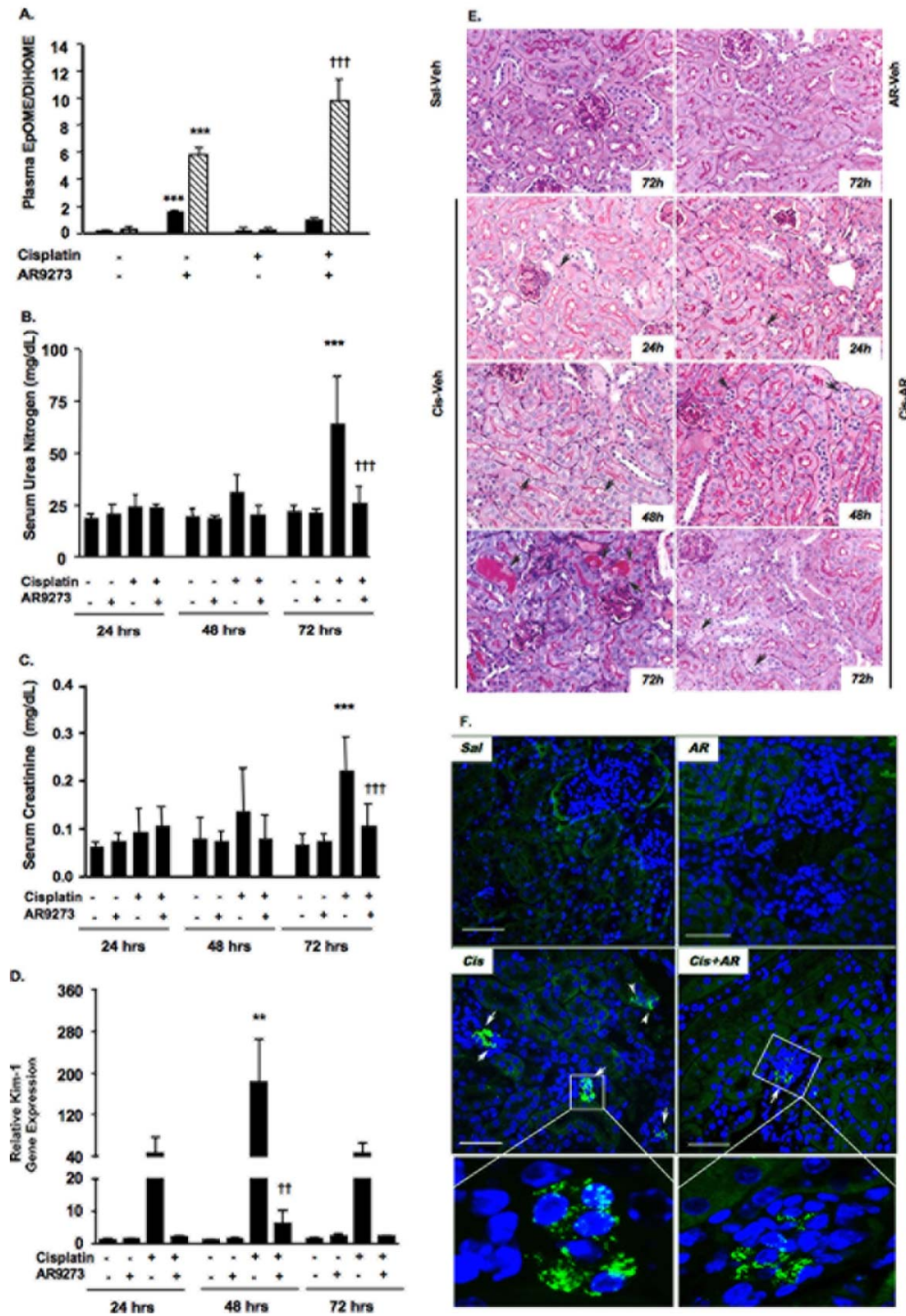


Figure 4.



**Figure 5.**

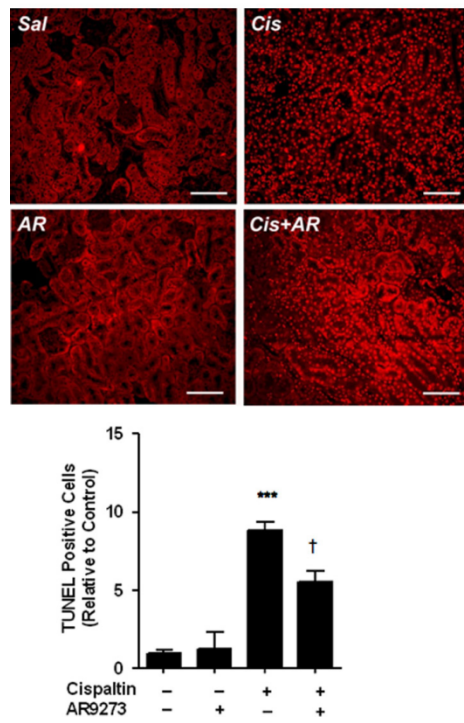


Figure 6.

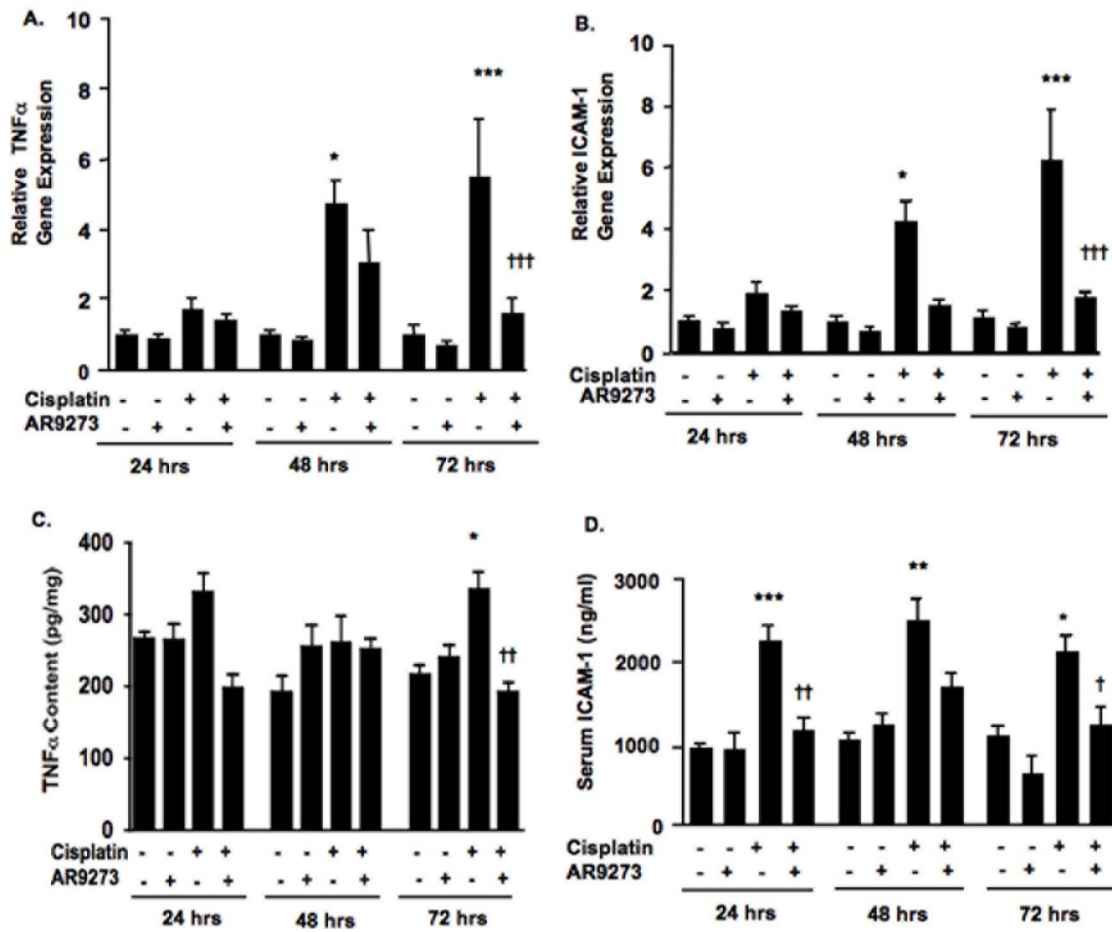
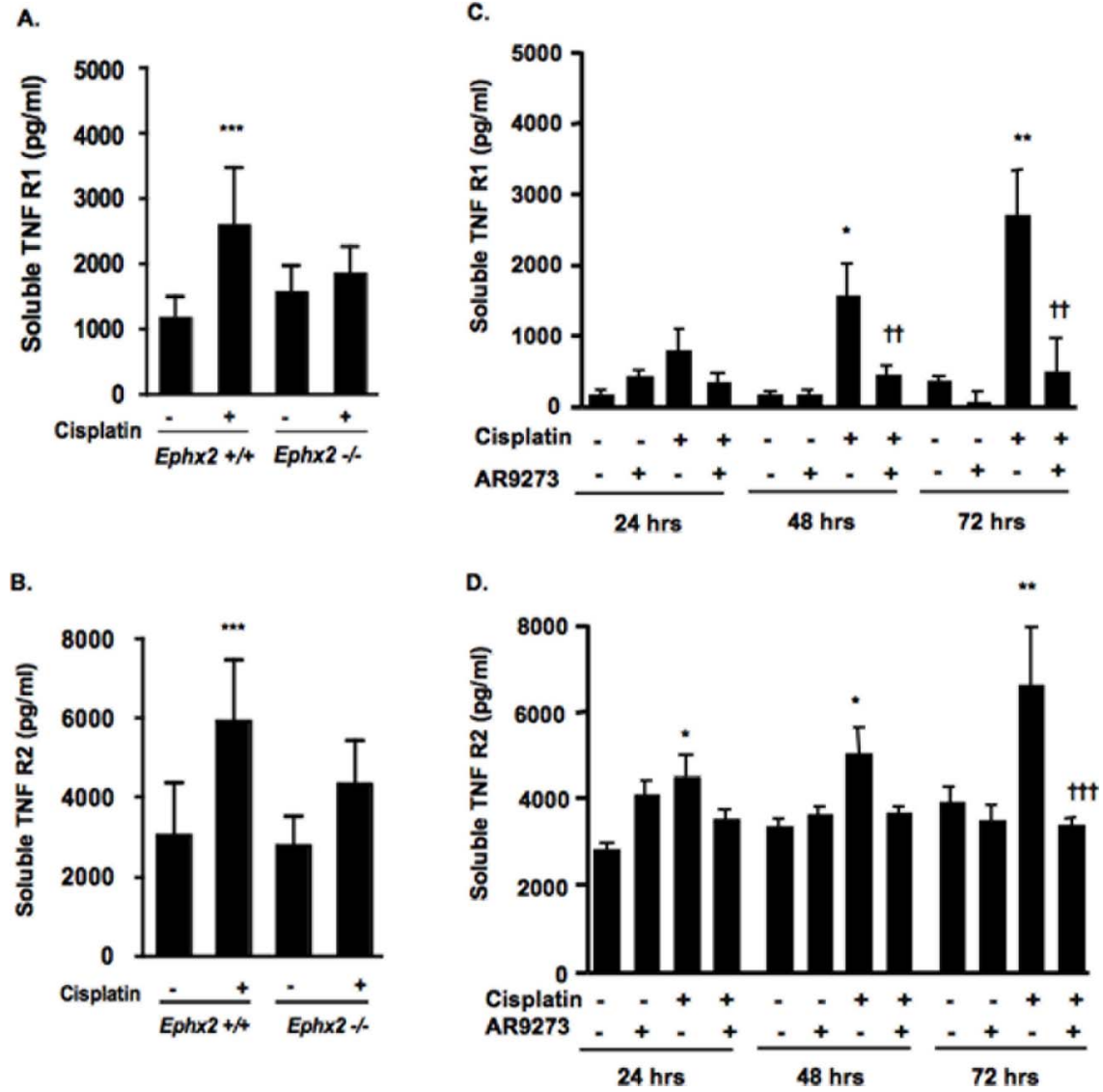


Figure 7.



**Figure 8.**

